Hindawi Publishing Corporation
Journal of Nanomaterials
Volume 2011, Article ID 348268, 15 pages
doi:10.1155/2011/348268

Research Article

Electrospun Collagen: A Tissue Engineering Scaffold with Unique Functional Properties in a Wide Variety of Applications

Balendu Shekhar Jha,[1] Chantal E. Ayres,[2] James R. Bowman,[3] Todd A. Telemeco,[4] Scott A. Sell,[5] Gary L. Bowlin,[2] and David G. Simpson[1]

[1] *Department of Anatomy and Neurobiology, Virginia Commonwealth University, Richmond, VA 23298, USA*
[2] *Department of Biomedical Engineering, Virginia Commonwealth University, Richmond, VA 23298, USA*
[3] *School of Medicine, Virginia Commonwealth University, Richmond, VA 23298, USA*
[4] *Division of Physical Therapy, Shenandoah University, Winchester, VA 22601, USA*
[5] *Physical Medicine and Rehabilitation Service, Hunter Holmes McGuire VA Medical Center, Richmond, VA 23249, USA*

Correspondence should be addressed to David G. Simpson, dgsimpso@vcu.edu

Received 1 October 2010; Accepted 9 February 2011

Academic Editor: Wei He

Type I collagen and gelatin, a derivative of Type I collagen that has been denatured, can each be electrospun into tissue engineering scaffolds composed of nano- to micron-scale diameter fibers. We characterize the biological activity of these materials in a variety of tissue engineering applications, including endothelial cell-scaffold interactions, the onset of bone mineralization, dermal reconstruction, and the fabrication of skeletal muscle prosthetics. Electrospun collgen (esC) consistently exhibited unique biological properties in these functional assays. Even though gelatin can be spun into fibrillar scaffolds that resemble scaffolds of esC, our assays reveal that electrospun gelatin (esG) lacks intact α chains and is composed of proinflammatory peptide fragments. In contrast, esC retains intact α chains and is enriched in the α 2(I) subunit. The distinct fundamental properties of the constituent subunits that make up esC and esG appear to define their biological and functional properties.

1. Introduction

Electrospinning has been used to fabricate a variety of polymers, including natural proteins [1–3], sugars [4], synthetic polymers [5, 6], and blends of native and synthetic polymers [7–9] into tissue engineering scaffolds composed of nano- to micron-scale diameter fibers, a size-scale that approaches the fiber diameters observed in the native extracellular matrix (ECM). The physical, biochemical, and biological properties of these unique biomaterials can be regulated at several sites in the electrospinning process. As this technology has matured, it has become apparent that many electrospun nanomaterials exhibit unusual, and often surprising, properties.

For many polymers, physical properties, including fiber diameter, pore dimension, and degree of scaffold anisotropy, can be regulated by controlling the composition of the electrospinning solvent, the air gap distance, accelerating voltage, mandrel properties, and/or the identity, concentration, and degree of chain entanglements (viscosity) present in the starting solutions [10–12]. The ability to directly manipulate these fundamental variables can have a dramatic impact on the structural and functional properties of electrospun materials. This is especially true when considering native proteins and blends of synthetic polymers and native proteins.

Collagen represents the most abundant protein of the mammalian ECM. As such, this natural polymer has long been used as a biomaterial in a variety of tissue engineering applications. This crucial ECM protein, as well as a variety of other native proteins, can be electrospun into fibers that resemble the native state [1]. Not surprisingly, the fibers of electrospun collagen do not appear to fully reconstitute the structural or mechanical properties of the parent material [12]. Simultaneously, it is unclear to what extent the electrospun analog "must" recapitulate the native material

to be a functional tissue engineering scaffold. The nature of the electrospun collagen fiber is the subject of debate and there are conflicting reports in the literature concerning its structural and functional properties [7, 12–15]. In this study, we compare and contrast the functional characteristics of electrospun collagen and electrospun gelatin (denatured collagen) in a variety of tissue engineering applications. We then explore how the procedures used to isolate and prepare collagen for the electrospinning process might ultimately impact its functional profile once it has been processed into a tissue engineering scaffold. We believe that it is essential to develop a more complete functional map of these novel materials to fully exploit them in the development of clinically relevant products.

2. Materials and Methods

2.1. Collagen Preparation. Collagen was isolated at 4°C. Calfskin corium (Lampire Biologics, Pipersville, PA) was cut into 1 mm^2 blocks and stirred for 24 hr in acetic acid (0.5 M), processed in a blender into a slurry, and stirred for an additional 24 hr. Solutions were filtered through cheesecloth, centrifuged at 10,000 × G for 12 hr; supernatant was recovered and dialyzed against ice cold, ultra pure 18 MΩ-cm water. Collagen isolates were frozen and lyophilized. Bovine gelatin Type B isolated from skin was purchased from Sigma (75 or 225 bloom).

2.2. Electrospinning: Collagen and Gelatin. Materials were purchased through Sigma unless noted. Lyophilized collagen (at 55 mg/mL) and gelatin (Sigma, 225 bloom at 110 mg/mL) were solubilized for 12 hr in 1,1,1,3,3,3-hexafluoro-2-propanol (HFP) and electrospun [1, 7, 10]. Conditions were adjusted to produce scaffolds composed of fiber diameters that were nominally 1 μm in cross-sectional diameter. Solutions were charged to 22 kV and delivered (3–7 mL/hr) across a 25 cm air gap. Electrospun samples, designated "recovered" electrospun collagen (rEC) or "recovered" electrospun gelatin (rEG) were produced by dissolving uncross-linked electrospun scaffolds immediately after spinning in ice cold, 18 MΩ-cm water; the final protein concentration was adjusted to 1.5 mg/mL. Collagen and gelatin starting electrospinning concentrations were manipulated to produce fibers of varying diameters. Where indicated, scaffolds were vapor cross-linked (1–12 hrs) in glutaraldehyde, blocked in 0.1 M glycine, rinsed in PBS, and disinfected in 70% alcohol prior to culture experimentation or implantation.

2.3. Cell Culture: Endothelial Cells. Electrospun scaffolds were cut into 12 mm diameter circular disks and cross-linked. A sterile 6 mm diameter glass cloning ring was placed on top of each disk and supplemented with 3,000 adult human microvascular endothelial cells (Invitrogen, C-011-5C) in a total volume of 100 μL. After 20 min the culture dishes were flooded with media to ensure that the cells were immersed. Cloning rings were removed after 24 hr of culture.

2.4. Cell Culture: Osteoblasts. Type I collagen and gelatin were electrospun across a 25 cm gap and directed at a grounded 6 in diameter circular steel plate. Tissue culture dishes were placed between the source electrospinning solutions and the grounded target to directly collect fibers on the culture surfaces. After cross-linking, equal numbers of osteoblasts (Clonetics, CC-2538) were plated onto each surface and cultured for 10 days in OBM basal media (CC-3208). As controls, cells were plated onto native tissue culture plastic or random gels composed of Type I collagen (Vitrogen: Cohesion Technologies), Simpson et al. [16]. For SEM imaging, osteoblasts were cultured directly on 6 mm diameter × 500 μm thick circular disks of electrospun collagen or gelatin (conditions optimized for 1 μm diameter fibers).

2.5. Dermal Reconstruction. Adult guinea pigs were brought to a surgical plane, fur was shaved and skin swabbed in betadine. Four 1 cm^2 full-thickness dermal injuries (complete removal of the dermis and hypodermis and bordered by the superficial fascia of the panniculus adiposus) were prepared on the dorsum of each animal. Injuries were treated with scaffolds composed of electrospun Type I collagen or gelatin (electrospinning conditions adjusted to produce scaffolds composed of fibers ranging from 250 nm to >2000 nm in average cross-sectional diameter). Scaffolds were vapor cross-linked to varying degrees. Each wound was treated with a candidate scaffold and covered with a piece of silver gauze that was sutured in place. Silver gauze remained in place for 5–7 days. Animals recovered on a warming pad and were provided with pain mitigation. Injuries were photographed at intervals. Data on wound closure was expressed as the percent injury surface area observed at the time of implantation. Representative samples were recovered for histological evaluation.

2.6. Muscle Fabrication. Three-day-old neonatal rats were decapitated, skin was removed. Skeletal muscle was removed, minced into 1 mm^2 pieces in sterile PBS and rinsed until clear of blood. Tissue was incubated in a sterile flask supplemented with 0.25% trypsin (Invitrogen) in a shaking (100 RPM) 37°C water bath. At 10 min intervals, tissue was cannulated and allowed to settle, and supernatant was removed and centrifuged at 800 × G for 6 min. Cell pellets were pooled in DMEM plus 10% FBS and 1.2% Antibiotic/Antimycotic (Invitrogen 15240). A 60 minute interval of differential adhesion to tissue culture plastic was used to reduce fibroblast contamination. Myoblasts were cultured for 3–5 days under conditions that minimized cell to cell contacts. In cell labeling assays, myoblast cultures were incubated in DiO (Invitrogen, L-7781) overnight according to manufacturer's recommendations.

Electrospun scaffolds were prepared on a 4 mm diameter round mandrel. With conditions optimized to produce 1 μm diameter fibers, cylindrical constructs were fabricated with a wall thickness of 200–400 μm [7]. Scaffolds were cross-linked. Myoblasts were recovered from culture and rinsed 2x in PBS by centrifugation (800 × G, 6 min). Electrospun

cylinders were sutured shut and suspended myoblasts were injected into the lumen of the constructs. Adult 150–180 gm Sprague Dawley rats were brought to a surgical plane. Fur on the hindlimb was shaved and skin was swabbed in betadine. In short-term studies (3 wks), a 4 mm × 15 mm long cylinder supplemented with cells was inserted directly into a channel ("intramuscular" position) prepared in the vastus lateralis muscle after the methods of Telemeco et al. [7]. In long term studies, a hemostat was passed deep to the quadriceps muscle group; engineered tissue (4 mm × 40 mm) was passed under the existing muscle mass and sutured (in an extramuscular position) to the proximal and distal tendons of origin and insertion for the quadriceps. Incisions were repaired, skin was stapled, and animals recovered on a warming pad.

2.7. Electrospinning: Nylon. To separate the fiber-forming properties of the different protein fractions from their fundamental biological properties, we applied collagen and gelatin fractions to electrospun scaffolds composed of nylon 66 (Ambion). Electrospun nylon has a high surface area and exhibits high protein binding capacity. Nylon was spun after the methods of Manis et al. [17]. Conditions were optimized to produce charged nylon fibers ranging 1.0–1.5 μm in diameter.

2.8. Cell Culture: Adult Human Dermal Fibroblasts. Dermal fibroblasts (HDF), (Cascade Biologics: C-013-5C) were passaged 3–5 times in basal dermal fibroblast medium 106 supplemented with a low serum growth kit (Cascade Biologics, S-003-K) prior to experimentation.

2.9. Cell Adhesion Assays. Electrospun nylon scaffolds were immersed in 20% methanol/phosphate buffered saline (PBS) [17], rinsed 3x in PBS and installed in a dot blotter manifold (Topac Model DHM-48). Wells were supplemented with 50 μL of collagen (control samples or fractions thermally denatured at 50, 60, 70, 80 or 90°C for 1 hr) or gelatin fractions containing equal amounts of protein. After 5 min, solutions were sucked through the membrane using a vacuum pump. Scaffolds coated with 1% bovine serum albumin (BSA) were used as controls. All wells were blocked with 100 μL of 1% BSA solution for 5 min and rinsed in PBS prior to use. In each assay, 3000 HDFs were suspended in 100 μL of media and applied to each surface for 1 hr at 37°C (dot blotter was used as a culture vessel; no vacuum was applied to the cell suspensions).

After the plating interval, the dot blotter was inverted to remove nonadherent cells, scaffolds were removed, rinsed in PBS, and fixed in ice cold methanol (20 min). For analysis, scaffolds were rinsed 5x in PBS plus 0.5% Triton, and incubated overnight at 4°C in primary goat antirabbit GAPDH antibody (Sigma # G9545, 1 : 5000). All antibodies were diluted in LiCor Odyssey Blocking Buffer (L-OiBB), and LOiBB plus 0.1% Tween-20 was used in all rinses. Cultures were rinsed 5x in L-OiBB, counter-stained with goat antirabbit IRDye 800 secondary antibody (LiCor 1 : 1000) for 1 hr and rinsed 5x. Data sets were captured at a line resolution of 169 μm using a Li-Cor Odyssey Infrared Imager. Adhesion was expressed as "Integrated Intensity" (signal-mm^2). Integrated intensity values were extrapolated to cell number using a standard curve of cells plated in parallel with the unknowns. Data sets were screened by one-way ANOVA ($P < .01$), Dunn's Method ($P < .05$), and a Mann-Whitney Rank Sum test ($P < .001$) was used in *post hoc* analysis. In cyclic RGD competition experiments, HDFs (10,000 cells per treatment) were incubated for 15 min at 37°C with 0.01, 0.1, or 1 μg/mL cyclic RGD peptide (Bachem, H-2574) or 1 μg/mL control RGD peptide (Bachem, H-4088). The cells were then plated for 1 hr on the different surfaces and were processed to image GAPDH as described.

2.10. Alpha Chain Analysis. Collagen samples were diluted to 0.15 mg protein/mL in Laemmli sample buffer and separated by SDS interrupted gel electrophoresis using 10% polyacrylamide gels. Gels were run until the dye front reached the base of the stacking gel, 1 mL of Laemmli buffer supplemented with 20% β-mercaptoethanol was added to the gel stacker and incubated for 30 min at room temperature. The separation run was then completed. Gels were stained with Coomassie brilliant blue overnight, de-stained and photographed. Densitometric analysis was conducted with NIH ImageJ software.

2.11. Cross-Linking Assays. See Newton et al. [12] for details of this assay. Percent cross-linking was calculated from the formula

$$\%\ \text{cross-linked} = 1 - \frac{\text{Abs}_c/\text{mass}_c}{\text{Abs}_{nc}/\text{mass}_{nc}}, \quad (1)$$

where Abs_c = absorbance of the controls at 345 nm; the unit of mass is given in mg. Abs_{nc} = absorbance of the unknowns at 345 nm; again the unit of mass is given in mg. All data is expressed as percent of cross-linking observed in electrospun scaffolds (controls) that have not been exposed to cross-linking reagents.

2.12. Scanning Electron Microscopy. Samples were sputter-coated and imaged with a Zeiss EVO 50 XVP scanning electron microscope (SEM) equipped with digital image acquisition. Average fiber diameter and pore area data was determined from representative samples using NIH Image-Tool (UTHSCSA version 3). All fiber diameter measurements were taken perpendicular to the long axis of electrospun fibers [10, 11].

2.13. Transmission Electron Microscopy. Samples were immersed in 2% glutaraldehyde for 12 hr at 4°C and postfixed in 1.0% osmium plus or minus 2.5% potassium ferricyanide [6, 7]. All samples were subjected to a graded series of dehydration and embedded in Poly/Bed (Polysciences).

3. Results

3.1. Functional Performance of Electrospun Collagen. To compare and contrast the biological properties of electrospun

collagen and electrospun gelatin, we conducted a series of *in vitro* and *in vivo* functional assays.

3.1.1. Endothelial Cell Growth. Critical to the bioengineering paradigm is the development of tissue engineering scaffolds that can support the proliferation and penetration of vascular elements. To evaluate this characteristic *in vitro,* we plated microvascular endothelial cells onto electrospun scaffolds of Type I collagen and electrospun gelatin composed of varying fiber diameters. During the initial plating phase, and over time in culture, cell shape, on both surfaces (collagen and gelatin), was modulated by the fiber size (and likely the pore characteristics that "travel" with the fiber size that is present in an electrospun scaffolds [10]) (Figure 1). Electrospun scaffolds of collagen and gelatin composed of small diameter fibers induced the expression of a highly flattened and stellate cell shape. This cell shape was retained throughout the culture interval on both surfaces (e.g., Figure 1 compare (a) = day 1 with (b) = day 7 as well as (i) and (j)). With increasing fiber diameter, the cells assumed a more rounded and elongated phenotype. After 10 days, microvascular endothelial cells cultured on collagen- or gelatin-based scaffolds with average cross-sectional fiber diameter less than about 1.0–1.50 μm remained on the dorsal surfaces of the constructs (Figure 1 (q), (r), (u) and (v)). As fiber size exceeded this threshold value and pore size increased to about 10,000 nm^2, the cells began to penetrate into the scaffolds (Figure 1 (s), (t), (w) and (x)). These results suggest that the physical arrangement of fibers (i.e., the pore characteristics) plays a role in regulating the infiltration of endothelial cells into an electrospun scaffold.

3.1.2. Osteoblast Differentiation. The 67 nm banding pattern typical of native Type I collagen is associated with the formation of nucleation and binding sites critical to the mineralization process in bone [18]. Superficially, electrospun fibers of collagen exhibit a similar structural motif. To examine the potential functional consequences of this motif, we plated osteoblasts onto surfaces coated with electrospun collagen and electrospun gelatin. Cultures plated onto surfaces coated with electrospun collagen exhibited low rates of proliferation and failed to form a confluent cell layer, even after 8 days. Phase bright crystals were present throughout these cultures (Figure 2). Cells plated onto surfaces coated with electrospun gelatin, Type I collagen gels, or native tissue culture plastic proliferated and formed a confluent cell layer over this same culture interval. Phase bright crystals were infrequently observed in any of these cultures. These data suggest electrospun collagen contains structural motifs necessary and sufficient to induce osteoblast differentiation and subsequent formation of hydroxyapatite crystals.

3.1.3. Dermal Reconstruction. From an architectural standpoint, tissue engineering electrospun scaffolds are theoretically very well suited for applications in dermal reconstruction. These constructs are deposited as nonwoven, fibrillar structures that exhibit an extensive void volume and pores that are completely interconnected with one another. To evaluate the efficacy of using electrospun collagen as a dermal template, we treated full thickness dermal injuries with various permutations of this material. To track the healing process, we measured total wound surface area as a function of treatment and time. We have used this metric because interventions that reduce wound contraction (as measured by an *increased* retention of wound surface area once the injury is healed) are associated with less scarring and more complete tissue regeneration [19].

In the first series of experiments, we treated wounds (1 cm^2) with dermal templates fabricated from electrospun collagen under conditions that produced fibers ranging 750–1,000 nm. These scaffolds were postprocessed to cross-link approximately 50% of the available sites. Wound closure took place in 16 days with these constructs (Figure 3(a)). When the extent of cross-linking was increased to 70% in these constructs, wound healing was delayed modestly and wound surface area was dramatically increased, a feature indicative of increased regeneration (Figures 3(a) and 3(c)). Histological examination of the tissue reconstituted with templates composed of electrospun collagen consistently revealed a smooth continuum of infiltrating cells. There were no overt signs of inflammation or fibrosis along the interface of the implanted templates and the adjacent uninjured tissue, regardless of the fiber diameter composition present in electrospun constructs of Type I collagen (Figures 4(a)–4(c)). Our tissue culture experiments demonstrated that the intrinsic architectural features present in an electrospun scaffold can modulate the extent to which endothelial cells can penetrate into these constructs. We observed a similar trend in our dermal reconstruction experiments. Injuries treated with templates composed of fibers less than 500 nm in diameter were less densely populated than templates composed of fibers greater than 750–1000 nm in diameter (Figure 4).

In parallel experiments conducted with a wide variety of electrospun scaffolds composed of gelatin (average fiber diameters ranging from 250 nm to approximately 3000 nm), we were unable to replicate these results. Wounds treated with electrospun gelatin consistently healed in the classic X shaped configuration (Figure 3(d)) that develops in response to wound contraction, this feature developed regardless of the fiber diameter or the degree of cross-linking present in the gelatin-based scaffolds. These scaffolds were consistently infiltrated by foreign body giant cells, indicating an inflammatory response to the implanted electrospun gelatin (Figures 4(d)–4(f)). These data indicate that architectural features and the biochemical identity of an electrospun scaffold composed of collagen interact to define its unique functional characteristics.

3.1.4. Muscle Engineering. To evaluate the efficacy of using electrospun collagen in a cell-based tissue engineering application, we used an *in situ* strategy to fabricate skeletal muscle prosthetics. In these experiments we electrospun Type I collagen onto a rotating 4 mm diameter mandrel; this resulted in the formation of a hollow cylinder with walls composed of 1 μm diameter fibers of electrospun collagen. These cylinders

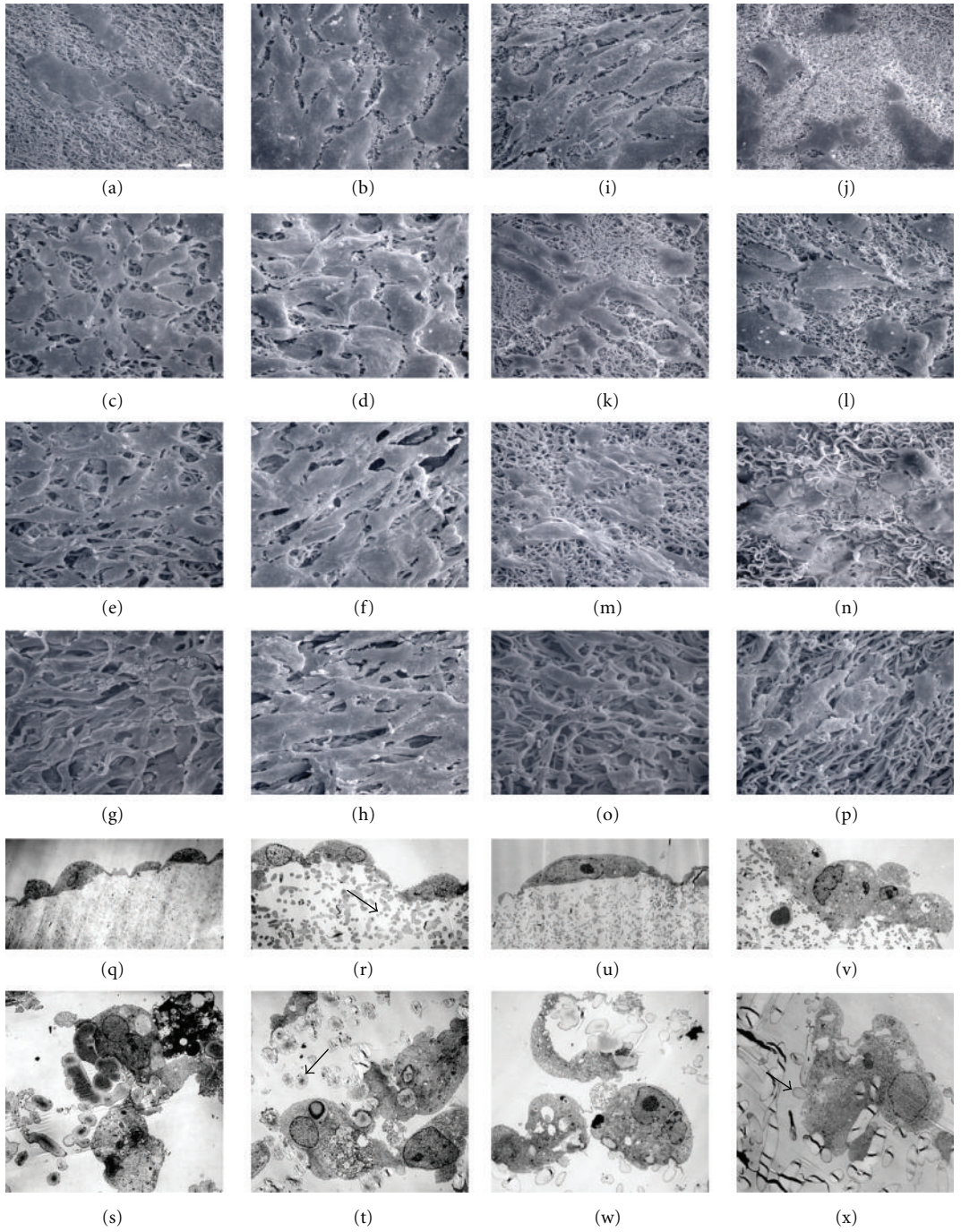

Figure 1: Endothelial interactions with electrospun collagen ((a)–(h)) and gelatin ((i)–(p)). Endothelial cell shape varied as a function of increasing fiber diameter on both electrospun collagen (Day 1: (a), (c), (e), (g) & Day 7: (b), (d), (f), (h)) and electrospun gelatin (Day 1: (i), (k), (m), (o) & Day 7: (j), (l), (n), (p)). Cell shape established during the early stages of plating persisted throughout the entire culture interval (e.g., for each scaffold cells at day 1 appeared to exhibit a similar cell shape after 7 days of culture). Cells expressed and retained a highly flattened and stellate shape when plated onto scaffolds composed of fibers less than 1,500 nm ((a)–(l)). At larger fiber sizes the cells exhibited a more elongated phenotype, this was especially evident on the collagen-based scaffolds ((e), (f), (g) and (h)). Penetration into the scaffolds was primarily regulated by average fiber diameter and pore size. TEMs of cross-sectional images of cells plated onto electrospun collagen ((q)–(t)) and electrospun gelatin ((u)–(x)) for 10 days. Average fiber diameters for collagen (a) & (q) = 449 ± 122 nm, (c) & (r) = 1,187 ± 297 nm, (e) & (s) = 1,886 ± 513 nm and (g) & (t) = 2,756 ± 855 nm. In gelatin (i) & (u) = 198 ± 50 nm, (k) & (v) = 491 ± 114 nm, (m) & (w) = 1,252 ± 302 nm, and (o) & (x) = 1,619 ± 414 nm (all fiber measurements from dry scaffolds prior to processing for cross-linking). Note that penetration was not evident until a nominal average fiber diameter of about 1,800 nm was achieved in the scaffolds (arrows in (r), (t), (x) indicate fibers in cross section). Scale bar in (a) = 20 μm.

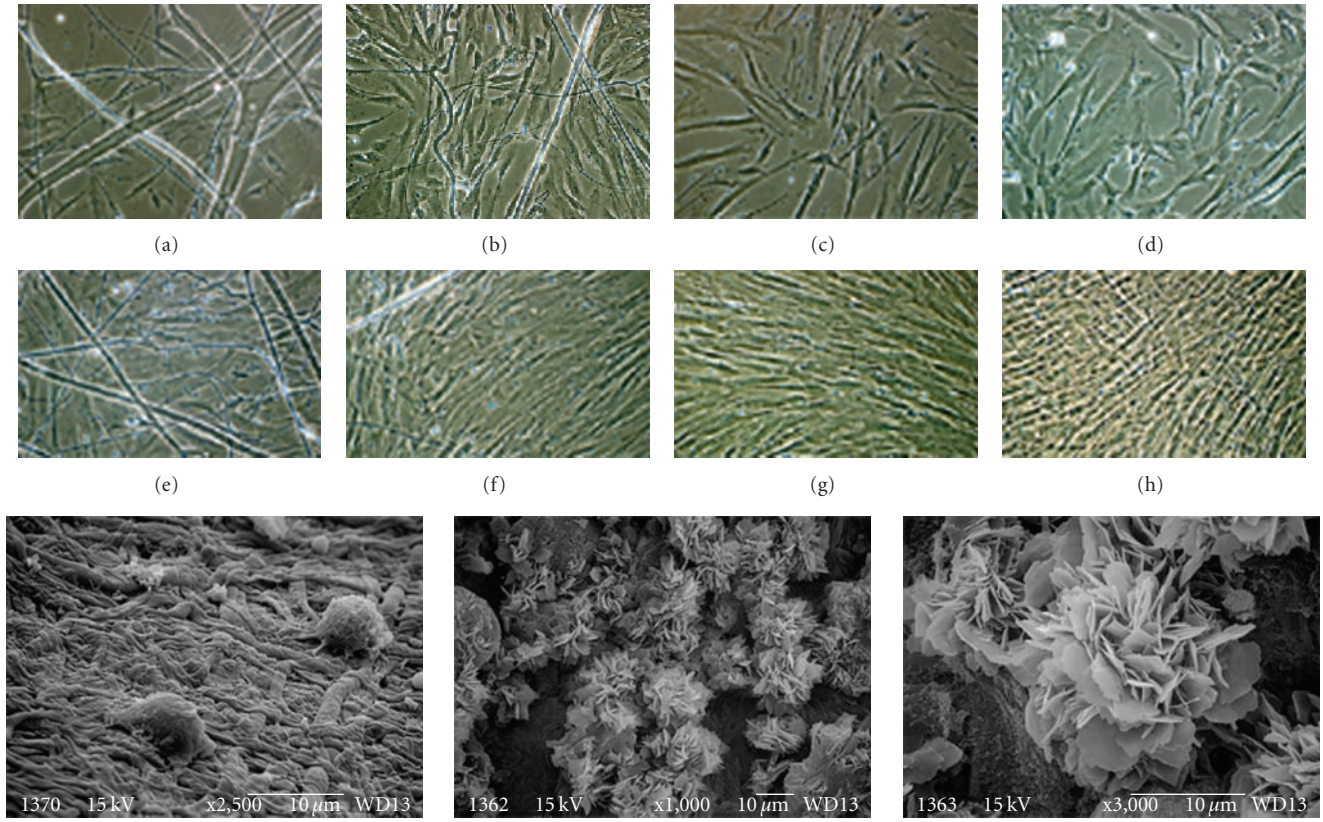

Figure 2: Osteoblast interactions with electrospun collagen and electrospun gelatin. Human osteoblasts plated for 1 (a)–(d) or 8 days (e)–(h). Cells plated on electrospun collagen ((a), (e)), electrospun gelatin ((b), (f)), collagen gel ((c), (g)), or tissue culture plastic ((d), (h)). Cells plated onto electrospun collagen remain subconfluent after 8 days of culture (e) and accumulated phase bright crystals. At the ultrastructural level, osteoblasts plated onto electrospun gelatin expressed a rounded cell shape (i); when plated onto electrospun collagen, the cells were covered with elaborate arrays of plate-like structures typical of hydroxyapatite crystals ((j), (k)).

were then supplemented with myoblasts and implanted directly into the vastus lateralis muscle. After 3 weeks, tissue fabricated with electrospun collagen was densely populated with cells. Nascent myotubes and functional blood vessels were evident throughout these implants (Figure 5). As with the dermal-templates, we observed a smooth continuum between the surrounding tissue and the engineered muscle with no evidence of fibrosis. In contrast to these results, tissue fabricated with gelatin based materials was necrotic, exhibited extensive fibrosis at the tissue interface and a massive infiltration of lymphocytes.

Given these results we next prepared engineered muscle tissue fabricated with electrospun collagen and directly sutured the constructs to the tendons of origin and insertion for the quadriceps muscle. These constructs were placed in an extramuscular position; in effect we are converting the quadriceps muscle into a "quintriceps" muscle. After 8 weeks, the engineered muscle was densely packed with fully differentiated myotubes that were distributed into stacked and linear parallel arrays that mimicked native tissue (Figure 6). This developing muscle tissue displayed well-formed myofibrillar elements. However, a range of cytoskeletal structural patterns was observed. For example, some areas of the tissue displayed loosely packed arrays of myofibrils (Figures 6(d) and 6(e)); other domains differentially took up the stains used to enhance contrast for light (Figure 6(g)) and transmission electron microscopy (Figure 6(h)). We suspect this differential staining is a reflection of protein density or protein identity with respect to the myofibrillar subunits. Collagen bundles were evident along the borders of the implanted tissue.

3.2. Analysis of Collagen Alpha Chain Structure and Function

3.2.1. Protein Analysis. We next conducted experiments to characterize how various processing conditions impact acid-soluble collagen and how these manipulations might regulate the evolution of the functional properties of an electrospun fiber. We first examined the effects of thermal denaturation on Type I collagen. These experiments were conducted to provide us with a benchmark for the evaluation of collagen structure and its α chain content in response to various steps in the electrospinning process. Collagen was isolated from calfskin corium using classical acid extraction methods,

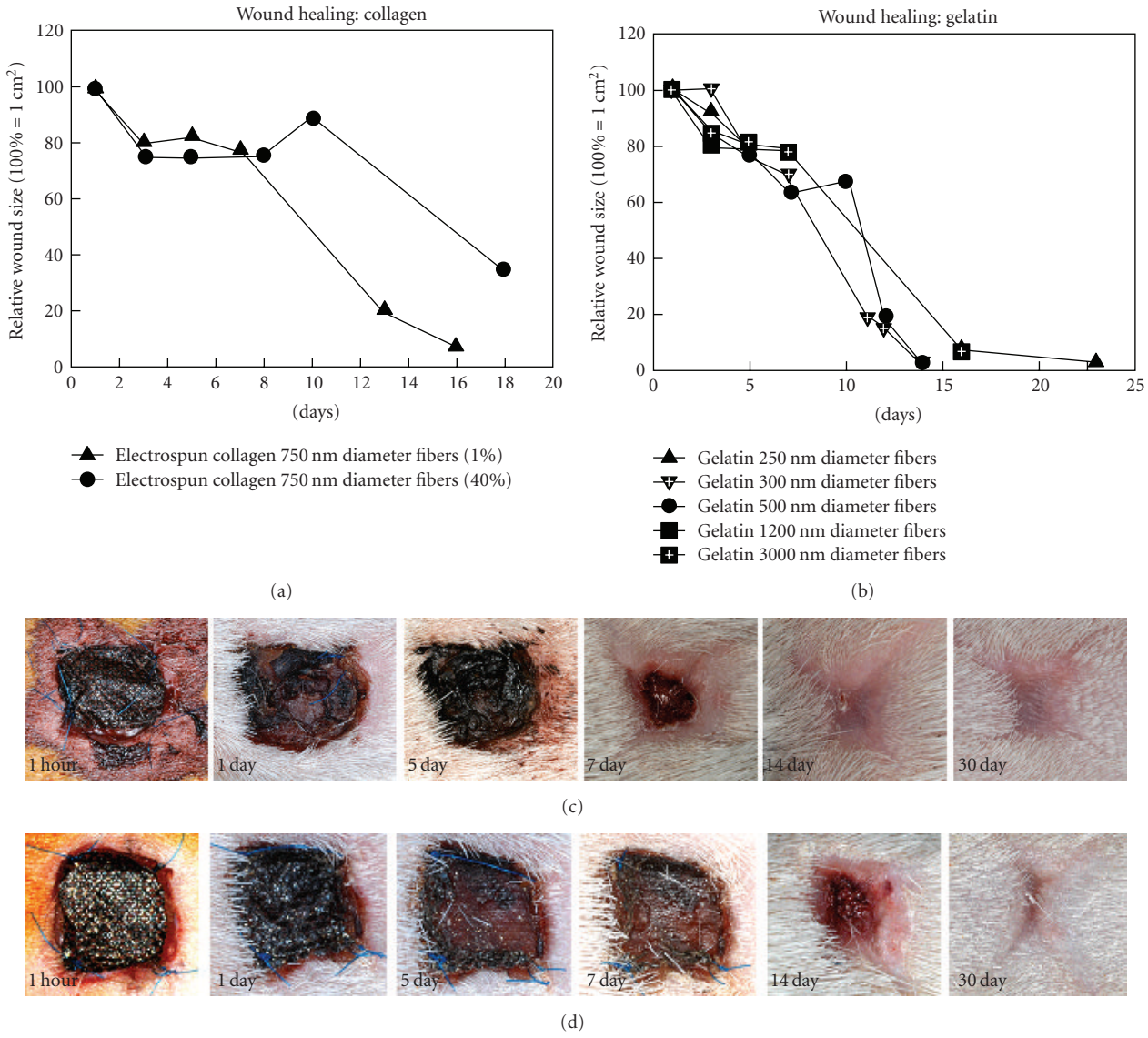

Figure 3: Dermal Reconstruction. Rates of wound closure in lesions treated with electrospun collagen (a) or electrospun gelatin (b). Note that increasing the extent of cross-linking has a modest effect on slowing wound closure and greatly increases total wound surface area in animals treated with electrospun collagen (a) and (c). Rates of wound closure were similar when injuries were treated with a wide variety of gelatin-based constructs (b) and (d). Panel (c) depicts the typical wound healing course for injuries treated with electrospun collagen in which approximately 70% of the available sites are cross-linked. Note the retention of wound surface area in this example. Panel (d) depicts the typical wound healing course for injuries treated with electrospun gelatin in which approximately 70% of the available sites are cross-linked. Note the classically X-shaped wound typical of a lesion that has undergone contraction.

a procedure routinely used to prepare collagen as a biomaterial and for use in the electrospinning process [1, 7]. Figure 7 illustrates an SDS gel depicting the α chain content of the acid soluble parent extract with respect to fractions that have been subjected to varying degrees of thermal denaturation.

Protein fractions were held at 4°C or heated to 50, 60, 70, 80, or 90°C for 1 hr. Detectable changes in the protein banding patterns present on the SDS gels were visible in all samples subjected to heating. Densitometric analysis of the separated protein fractions revealed that 50% of the collagen α chains were lost within 1 hr when soluble collagen was exposed to 70°C (Figure 7). Exposure to higher temperatures accelerated the loss of the collagen α chains from the soluble fractions and resulted in progressively more α chain fragmentation and smearing in the gel lanes typical of a sample that has been broken down into a heterogeneous mixture of peptides. At temperatures of 80°C and greater, the protein bands corresponding to the individual α chains were completely lost after the 1 hr incubation interval. Commercially procured gelatin (collagen that has been heated and denatured during isolation) samples exhibited little or no protein banding associated with intact α chains on the SDS gels; these samples ran nearly exclusively as a continuous smear of proteins (not shown, see [7]).

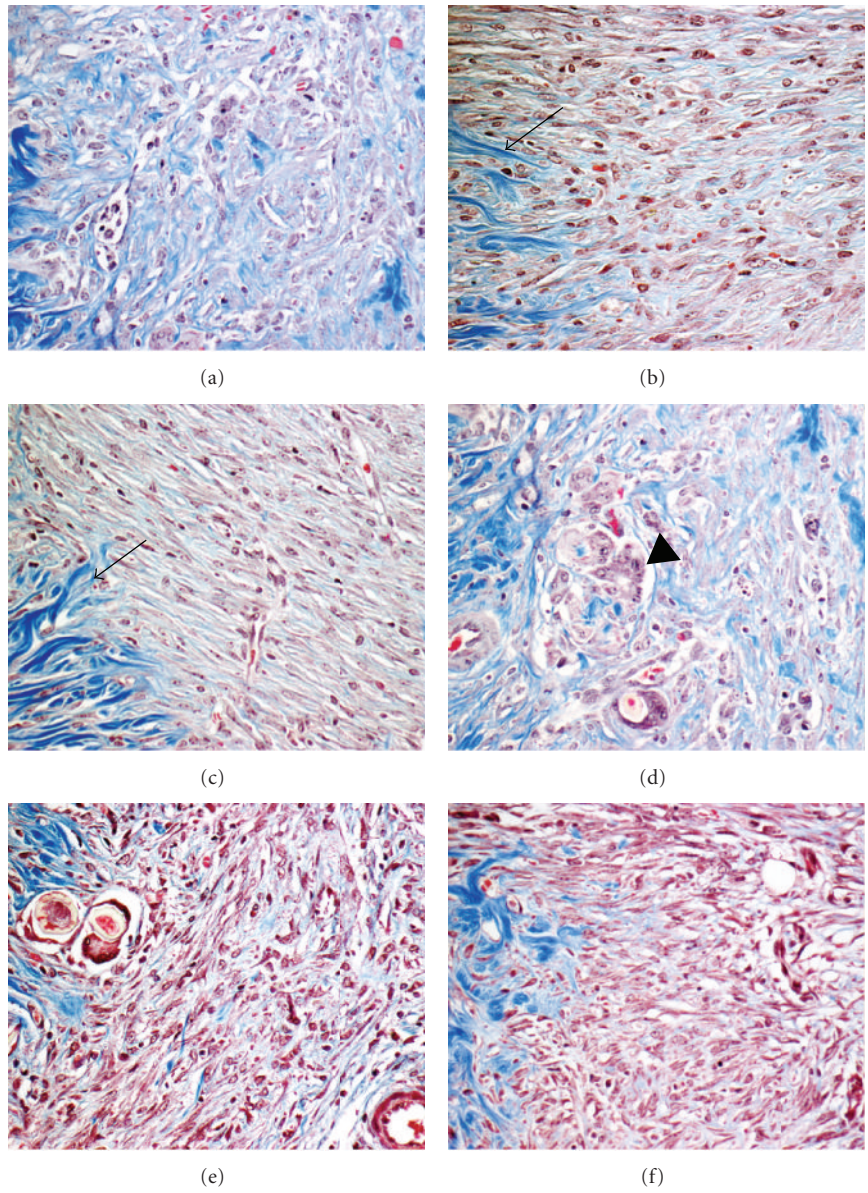

Figure 4: Dermal Reconstruction. Healing response to electrospun collagen (a)–(c) and electrospun gelatin (d)–(f) as a function of fiber diameter and pore dimension. Collagen-based implants exhibited a smooth continuum of cells at the interface of the lesion and the surrounding tissue. In each of the images depicted in this figure, native, uninjured tissue appears to the left of each data image (delineated by the large blue staining collagen bundles in the histological preparations, arrows (b) and (c)). Gelatin based-scaffolds were consistently less heavily infiltrated and exhibited evidence of an inflammatory response and accumulated foreign body giant cells (arrow head (d)). (a) and (d) average fiber diameter = 240–280 nm, average pore dimension =1500–2000 nm^2, (b) and (e) average fiber diameter 500–600 nm, average pore dimension 3000–5000 nm^2, (c) and (f) average fiber diameter 800–1000 nm, average pore dimension 4000–5000 nm.

To examine how the electrospinning process (solvents, electric field, and the flash-lyophilization of proteins that occurs during fiber formation) might alter collagen α chain content, we next prepared scaffolds composed of electrospun Type I collagen or commercially sourced gelatin (conditions optimized to produce average fiber diameters = 1 μm). As judged by scanning electron microscopy, these scaffolds were superficially identical. However, transmission electrospun microscopy reveals that scaffolds of electrospun collagen exhibit the 67 nm banding pattern typical of the native fibril (Figures 8(a)–8(d)). In contrast, fibers of the electrospun gelatin lack this distinctive structure and are nearly homogenous in appearance.

For protein characterization of the electrospun scaffolds, we redissolved the collagen and gelatin-based scaffolds and separated the resulting extracts by SDS gel electrophoresis. The protein banding patterns on the gels and the specific compliment of α chains in the electrospun collagen and

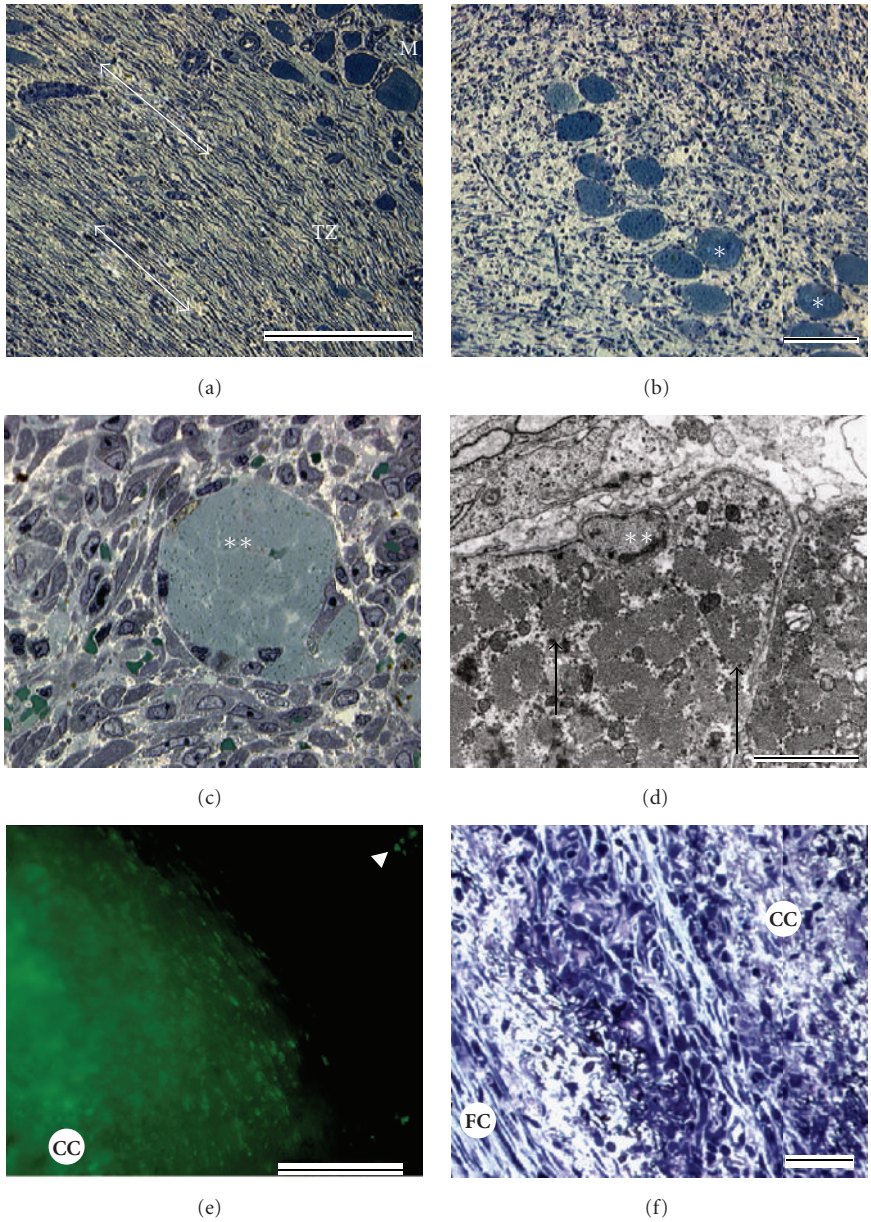

Figure 5: Muscle Fabrication: 3 Weeks. (a) Cross-section through the wall of cylindrical construct placed within the tissue of the rat vastus lateralis. M = endogenous host muscle tissue, TZ = transitional zone occupied by the wall of the electrospun construct. Note the lack of a fibrotic capsule. ((b), (c)) Sections taken from within the lumen of the tissue, dense cell populations are evident as are nascent myotubes (*). Scattered vascular elements are apparent and intermingle with the surrounding cell population. (d) TEM cross-section of developing myotube with forming myofibrillar elements (arrows). (e) Cell labeling experiments indicate that few cells migrate out of the implanted tissues (arrowhead). The bulk of the labeled cells are retained within the lumen of the electrospun constructs. (f) Tissue fabricated from gelatin undergoes necrosis and develops a fibrotic capsule (FC). CC = central core of implant.

the control starting material (Acid soluble Type I Collagen: Figure 7) were similar, but not identical. Samples of electrospun collagen exhibited subtle derangements in α chain content and, as judged by densitometric analysis, it was enriched in the $\alpha 2$ (I) content (see Figure 7) with respect to the other α chains. Protein separation analysis of the electrospun gelatin revealed, as expected, nearly complete α chain fragmentation (these samples displayed complete fragmentation even prior to the electrospinning process) and was comparable to the calfskin collagen samples heated to 90°C for 1 hr (Figure 7).

3.2.2. Alpha Chain Functional Properties. Next we examined how thermal manipulation impacted the adhesion properties of acid-soluble collagen and its electrospun variants. In these experiments, we coated electrospun fibers of charged nylon with equal amounts of the various protein fractions described in Figure 7. This strategy made it possible to

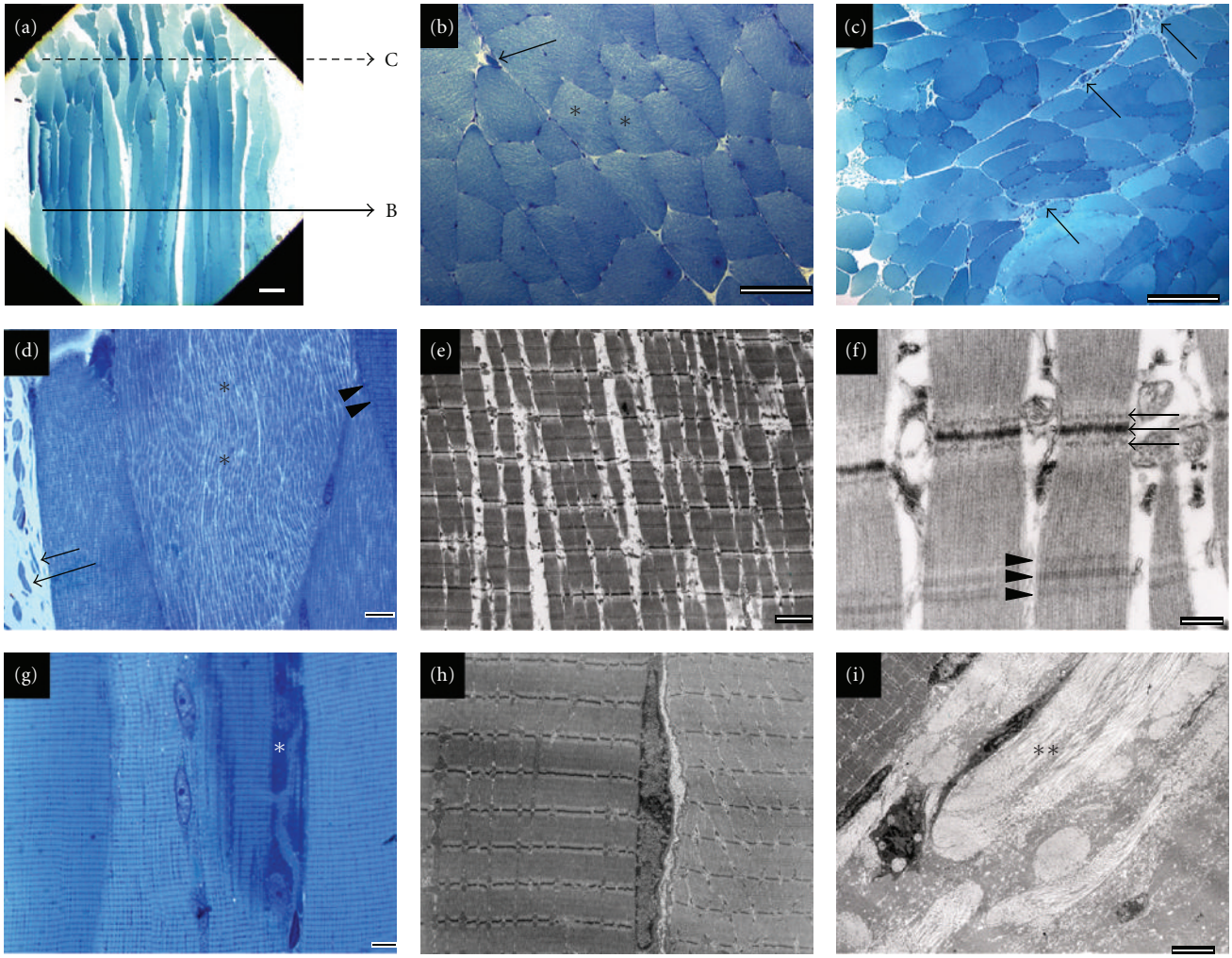

Figure 6: Muscle Fabrication: 8 Weeks. (a) Low magnification survey image depicting the terminal portions of muscle tissue engineered *in situ*. Images depicted in panels (b) and (c) were taken from the cross-sectional area denoted as "B" and "C", respectively in panel (a). The tissue distal to the attachment sites exhibited stacked arrays of myotubes ((b), asterisks). Tissue alignment is disrupted to some degree at the distal attachment sites as a consequence of the sutures used to place the tissue ((c), arrows indicate functional blood vessels). Myofibril density is observed to vary within cells that are in close proximity to one another ((d), arrowheads and asterisk; also the myofibrillar density in (d) and (e) to (g) and (h)) and some subdomains of the tissue stain differentially at both the light (g) and EM levels (h) with stains designed to enhanced contrast. The tissue is highly biosynthetic as evidence by the accumulation of proteins in the vicinity of the nuclei and golgi (g, asterisk). A subset of engineered tissue exhibits sarcomeres (f) with unusual cytoarchitectural patterns at the Z bands (arrows) and H zones (arrowheads) characterized by accessory electron dense structures. At the ultrastructural level, the implants are surrounded by collagen fibrils ((i) asterisks).

separate the fiber-forming capacity of each fraction from the biological activity that it displayed while presenting each fraction in a "matrix" that exhibited identical architectural patterns (fiber size, pore properties, and material properties). Equal numbers of dermal fibroblasts were then plated onto protein-coated electrospun nylon fibers. Rates of adhesion to the parent collagen fraction were approximately 50% greater than rates of adhesion to BSA-coated surfaces (Figure 8(e)). With one exception, thermal manipulation of the acid-soluble collagen fractions did not dramatically impact functional performance in these assays. Samples heated to 70°C supported substantially higher rates of adhesion than the BSA-coated surfaces and all of the other collagen fractions ($P < .002$), the gelatin samples ($P < .001$), and the samples recovered from electrospun scaffolds ($P < .001$). Rates of adhesion to Type I collagen recovered after electrospinning were not statistically different from the parent controls and were qualitatively much higher than gelatin and the electrospun gelatin samples.

The denaturation of collagen α chains uncovers RGD binding sites [20, 21]. To test for the presence of these sites in the different samples, we challenged cells in the adhesion assays with increasing amounts of cyclic RGD peptide. The RGD peptide reduced adhesion in the control samples by about 20% and nearly 60% in collagen samples that been heated to 70°C. No inhibition was detected in the collagen

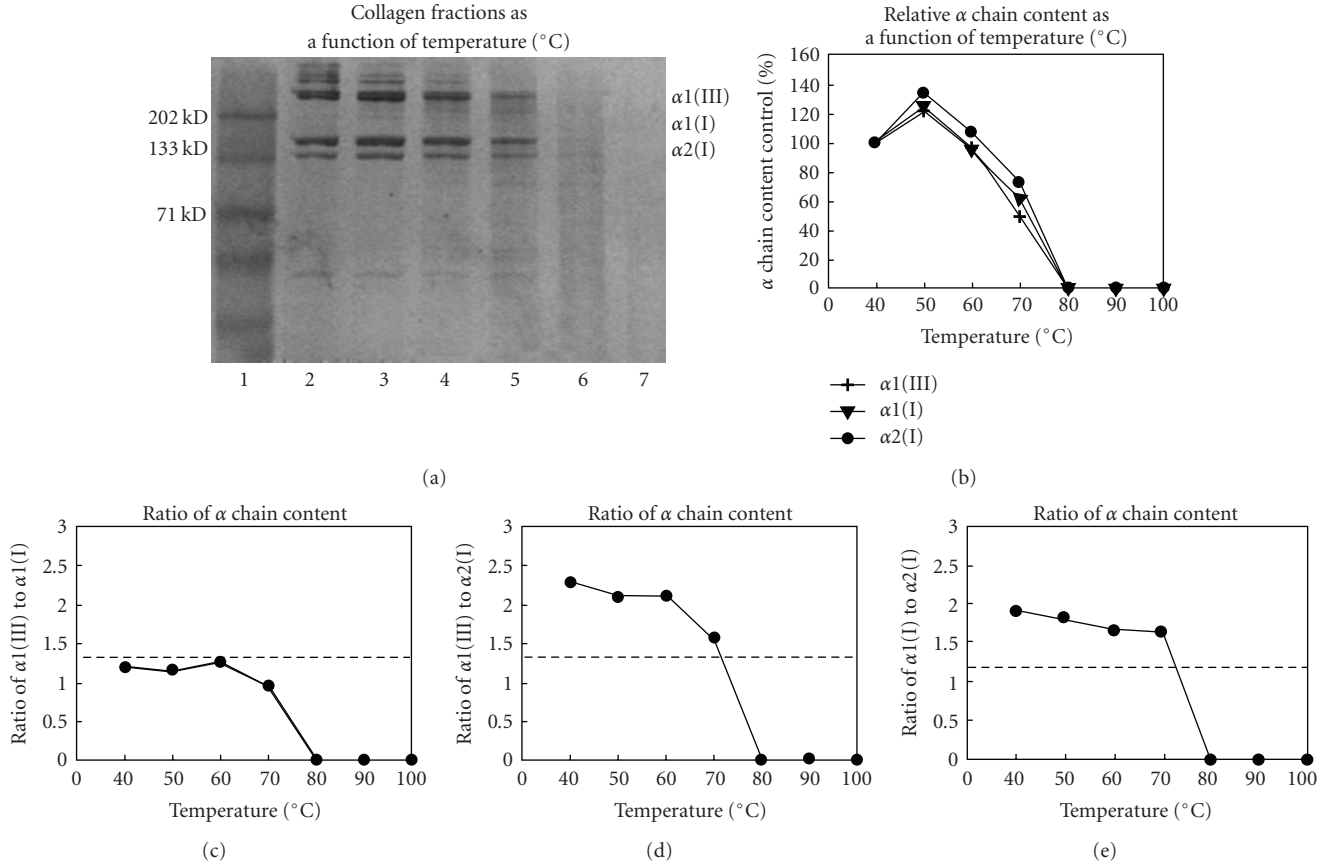

FIGURE 7: Analysis of Type I collagen α chain content. (a) Representative SDS gel depicting the affect of various degrees of heat denaturation on soluble collagen. Lane 1 = MW standards, 2 = control sample maintained and stored at 4°C, 3 = sample heated to 50°C for 1 hr, 4 = 60°C, 5 = 70°C, 6 = 80°C, and 7 = 90°C. (b) Densitometric analysis of α chain content from denaturation experiments. (c) Densitometric analysis (c) ratio of α 1(III) to α 1(I), (d) ratio of α 1(III) to α 2(I), (e) ratio of α 1(I) to α 2(I) as a function of thermal insult. Dotted lines in (c)–(e) depicts the actual ratio of the α chains present in collagen recovered immediately after electrospinning (no thermal insult).

recovered after electrospinning (Figure 8(f)). It is clear from the RGD-based competition assays that collagen recovered after electrospinning behaves very differently than denatured collagens or material recovered from a scaffold of electrospun gelatin. This observation is relevant when considering the functional properties of an electrospun collagen fiber that appears to lack the 67 nm repeat banding pattern. As long as the α chains are intact, even if they are not arrayed into a polymeric form that exhibits the 67 nm repeat banding pattern, these fibers can be expected to exhibit unique and potent biological properties. Together, our SDS gel assays and adhesion results indicate that electrospinning does not directly denature collagen α chains.

4. Discussion

In this study, through our functional assays, we explored the biological properties of electrospun collagen and electrospun gelatin. These two materials (collagen and gelatin) consistently exhibited very different functional profiles in all our assays. We note that endothelial cells began to penetrate into the fiber arrays of both electrospun collagen and electrospun gelatin once a critical fiber/pore threshold was reached. However, subjectively cell growth appeared to be much more rapid on the collagen-based scaffolds. We conclude from these *in vitro* experiments, in the absence of an inflammatory cascade or other antigenic complications, that endothelial cell infiltration is not limited by scaffold composition. Rather, gross structural properties are more important in this type of setting. The composition of the scaffolds appeared to dictate more subtle functional characteristics that regulated cell growth.

Cell culture experiments conducted with osteoblasts indicate that fibrils of electrospun collagen appear to be sufficient to induce differentiation and promote the accumulation of hydroxyapatite crystals *in vitro*. We believe this rather unexpected result may be a reflection of an intrinsic structural motif that is uniquely present in electrospun collagen. We did not observe this same result when we plated cells onto a collagen gel, a form of collagen that normally self-assembles into fibrils that contain a repeating banding pattern that also mimics native collagen [22]. Since both electrospun collagen and the fibers present in a collagen gel can exhibit a banding pattern, it is unclear

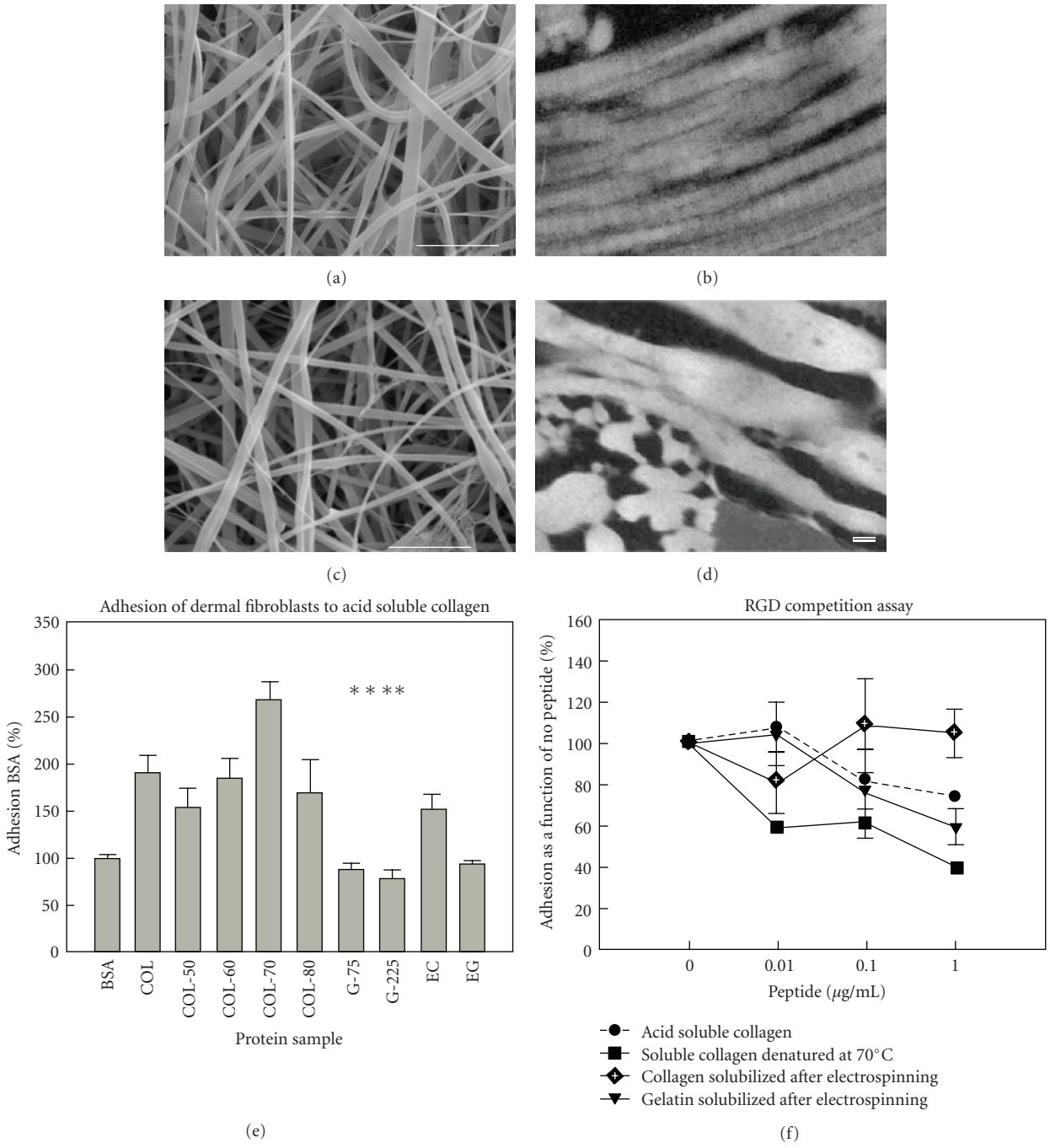

Figure 8: Ultrastructural and functional characteristics of collagen. Representative scanning electron and transmission electron micrographs of electrospun collagen ((a), (b)) and gelatin ((c), (d)). (e) Cell adhesion to various forms of collagen; maximal adhesion was observed in samples heated to 70°C. (F) RGD competition binding assay. Cyclic RGD peptides inhibited adhesion to denatured collagens in a concentration-dependent manner and had minor effects on control acid-soluble starting material and no effect on collagen recovered from electrospun scaffolds. Scale bars in (a) and (c) = 10 μm. Scale bar in (d) for (b) and (d) = 100 nm.

what drives these results. It is clear that these two types of fibers have subtle structural differences; fibers of electrospun collagen are not stable in an aqueous environment, unless they are cross-linked. In contrast, the fibers of a collagen gel are fully stable under these conditions and do not require such treatment. Fiber stability in a collagen gel is linked to the exothermic reaction that occurs during fiber polymerization; this leads to the partial denaturation of the constituent α chains and results in a more stable fiber structure. In the electrospinning process, collagen alpha chains essentially undergo flash lyophilization. These inherent differences in the fiber formation process likely result in

the production of fibers exhibiting very different fine structures.

In dermal applications, wounds treated with electrospun collagen and electrospun gelatin underwent resolution over a similar time course. The nature of the tissue that resulted at the conclusion of wound closure was very different and varied as a function of fiber composition and the extent of cross-linking that was introduced in the scaffolds. Injuries treated with lightly cross-linked electrospun collagen and all samples of electrospun gelatin underwent varying degrees of wound contraction. Introducing additional cross-linking into the collagen-based materials likely stiffens the constructs and makes them less susceptible to wound contraction. All of the collagen-based scaffolds were infiltrated by fibroblasts and exhibited numerous functional blood vessels. In contrast, injuries treated with electrospun gelatin were consistently less densely populated and showed an accumulation of foreign body giant cells at the borders of the wound. This adverse response in the gelatin-based materials is undoubtedly related to the proinflammatory peptides present in highly denatured collagens [23].

The essential capacity of electrospun collagen to support rapid cell infiltration was readily apparent from the experiments in which we fabricated skeletal muscle *in situ*. The interconnected nature of the pores present in a scaffold of electrospun collagen appears to provide more than enough passive nutrient exchange to support the donor cell population. A nascent vascular supply developed in tandem with muscle differentiation to support the increased metabolic demand associated with this process. Consistent with this conclusion, we observed functional blood vessels traversing the external walls of the implanted tissue and penetrating into the internal aspects of the constructs. In contrast, once again, tissue fabricated with electrospun gelatin induced a marked inflammatory response, and by 3 weeks the tissue was largely necrotic.

To develop an understanding of the basis of biological properties of electrospun collagen, we compared and contrasted the structure and function of collagen α chains in samples subjected to varying degrees of thermal denaturation and electrospinning. Not surprisingly, α chain content is dramatically altered in response to heating. At 70°C for 1 hour, 50% of the α chains are lost; at 80°C there is essentially complete α chain fragmentation and specific bands corresponding to α1(III), α1(II), and α2(I) are no longer detectable. The α chain content of collagen subjected to electrospinning is subtlety altered from the pattern observed in the starting materials (acid-soluble collagen). Based on our analysis,we have concluded that electrospun samples become enriched in α2(I) content. This conclusion is based on the observation that the ratio of α1(III): α1(I) is normal in the electrospun samples, α1(III): α2(I) is reduced and α1(I): α2(I) is reduced. Since the ratio of α1(III): α1(I) is unchanged we must assume that no change in α1(III) content has occurred as a consequence of the electrospinning process. Given this assumption and the observation that both α1(III): α2(I) and α1(I): α2(I) are depressed; the common factor is a change in α2(I) content; an increase in α2(I) is the simplest explanation for the observed results. As the denominator in both ratios, any increase in α2(I) content results in a decrease in these ratios. It is unclear how this enrichment may occur; it is possible that differences in alpha chain solubility (or stability) in the electrospinning solutions may exist, leading to a preferential enrichment of the α2(I) chain. This result awaits further investigation.

Our baseline adhesion experiments failed to definitively identify a specific binding profile that might be used to evaluate the functional profile of the collagen α chains. A number of integrins ($\alpha1\beta1$, $\alpha2\beta1$, $\alpha3\beta1$) bind to Type I collagen in an RGD-independent manner and the $\alpha v\beta3$ integrin binds with high affinity to *denatured* collagen in an RGD-dependent manner [21]. In competition binding assays, RGD challenge had little or no effect in control samples of collagen or collagen that had been recovered after electrospinning, suggesting that electrospinning in and of itself does not induce damage in a fashion that specifically uncovers cryptic RGD binding sites. We saw a dramatic decrease in adhesion when these same experiments were conducted with collagen fractions that had been heated to 70°C, these samples exhibited clear evidence of denaturation in our SDS gel studies.

5. Conclusions

Biophysical and structural evaluations demonstrate that electrospinning does not truly reconstitute the native structure of the collagen fibril [13]. Additionally, our data suggests that fibers of electrospun collagen become enriched in α2(I) content. However, our functional assays demonstrate that electrospun collagen has unique biological activity in a wide variety of tissue engineering applications. These data argue that it is not necessary to fully recapitulate the structure of the native fibril to generate a biologically relevant tissue engineering scaffold.

We believe that there are likely three critical variables that ultimately interact to determine the structural and functional properties of the electrospun collagen fibril. These include the quality of the starting material, the specific electrospinning conditions and, finally, the postprocessing manipulations that are used to prepare the material for use in a tissue engineering application. The first consideration is paramount; the starting material must not be denatured during any of the processes used to isolate and prepare the collagen for electrospinning (acid extraction, centrifugation steps, lyophilization and storage). The use of partially denatured collagen will obviously compromise the functional profile of the final product. Gelatin, a material that is composed of highly fragmented peptides readily spins into fibers but, it is highly proinflammatory in many settings.

Second, the role of fiber size in the formation of the ultrastructural organization of electrospun collagen has not been explored to any extent. The 67 nm banding pattern observed in electrospun samples appears to be most prominent in constructs composed of small diameter fibers. Some laboratories report that this banding pattern is confined to relatively small domains in an electrospun scaffold or that it is absent altogether [13]. We would argue that

the 67 nm repeat does not have to be present to impart potent functional properties onto the electrospun collagen fiber. Our cell adhesion experiments demonstrated that native and denatured collagen α chains have very distinctive biological properties, even when they are not assembled into fibrils. Given the dramatic differences in performance that distinguish electrospun collagen from electrospun gelatin in a broad spectrum of tissue engineering applications, it seems premature to discount the functional significance of this material [13].

Finally, during electrospinning collagen α chains are subjected to a very high strength electric field. This electric field must place these peptides in a high energy state as they traverse the charged electrospinning field; these protein subunits are then frozen and trapped in this high energy state by the flash lyophilization process that makes fiber formation possible. This residual energy may have direct role in determining the fine structure (banding) of the resulting fibers. Electrospun fibers of collagen that have been modestly cross-linked will undergo coiling when placed into an aqueous solution; this coiling is dramatically reduced as a function of increasing degrees of cross-linking [12]. At very high levels of cross-linking, fibers of electrospun collagen retain a nearly linear conformation when hydrated.

Modest cross-linking conditions appear to stabilize gross fiber structure (sufficient to keep the fibers from dissolving in an aqueous buffer); however, a modest degree of cross-linking does not appear to be sufficient to completely suppress α chain reorganization as these subunits return to a basal energy state. Upon hydration, the shedding of this excess energy appears to drive coiling. At high levels of cross-linking, fibril coiling is suppressed, suggesting the α chains are trapped in a very different tertiary configuration as compared to the fibers of more modestly cross-linked structures that can undergo molecular reorganization. The potential contribution of these variables in the formation of structure, and functional considerations in the electrospun collagen fibril, awaits further investigation. Given the potent biological activity of electrospun collagen, in a broad spectrum of applications, we can anticipate the development of unique tissue engineering scaffolds and the introduction of a new generation of tissue engineering products in the clinical market place.

Acknowledgments

This study is supported in part by NIH EB003087 (Simpson) and USAMRMC 9918006 (Simpson). Electron microscopy was conducted at the VCU Department of Neurobiology and Anatomy Microscopy Facility, supported in part by NIH-NCRR Shared Instrument Grant (1S10RR022495) and NIH-NINDS Center Core Grant (5P30NS04763).

References

[1] J. A. Matthews, G. E. Wnek, D. G. Simpson, and G. L. Bowlin, "Electrospinning of collagen nanofibers," *Biomacromolecules*, vol. 3, no. 2, pp. 232–238, 2002.

[2] C. P. Barnes, M. J. Smith, G. L. Bowlin et al., "Feasibility of electrospinning the globular proteins hemogloblin and myoglobin," *Journal of Engineered Fibers and Fabrics*, vol. 1, no. 2, pp. 16–28, 2006.

[3] M. McManus, E. Boland, S. Sell et al., "Electrospun nanofibre fibrinogen for urinary tract tissue reconstruction," *Biomedical Materials*, vol. 2, no. 4, pp. 257–262, 2007.

[4] S. W. Rothwell, E. Sawyer, J. Dorsey et al., "Wound healing and the immune response in swine treated with a hemostatic bandage composed of salmon thrombin and fibrinogen," *Journal of Materials Science*, vol. 20, no. 10, pp. 2155–2166, 2009.

[5] E. D. Boland, B. D. Coleman, C. P. Barnes, D. G. Simpson, G. E. Wnek, and G. L. Bowlin, "Electrospinning polydioxanone for biomedical applications," *Acta Biomaterialia*, vol. 1, no. 1, pp. 115–123, 2005.

[6] B. S. Jha, R. J. Colello, J. R. Bowman et al., "Two pole air gap electrospinning: fabrication of highly aligned, three-dimensional scaffolds for nerve reconstruction," *Acta Biomaterialia*, vol. 7, no. 1, pp. 203–215, 2011.

[7] T. A. Telemeco, C. Ayres, G. L. Bowlin et al., "Regulation of cellular infiltration into tissue engineering scaffolds composed of submicron diameter fibrils produced by electrospinning," *Acta Biomaterialia*, vol. 1, no. 4, pp. 377–385, 2005.

[8] S. A. Sell, M. J. McClure, C. P. Barnes et al., "Electrospun polydioxanone-elastin blends: potential for bioresorbable vascular grafts," *Biomedical Materials*, vol. 1, no. 2, pp. 72–80, 2006.

[9] M. J. McClure, S. A. Sell, C. E. Ayres, D. G. Simpson, and G. L. Bowlin, "Electrospinning-aligned and random polydioxanone-polycaprolactone-silk fibroin-blended scaffolds: geometry for a vascular matrix," *Biomedical Materials*, vol. 4, no. 5, 2009.

[10] C. Ayres, G. L. Bowlin, S. C. Henderson et al., "Modulation of anisotropy in electrospun tissue-engineering scaffolds: analysis of fiber alignment by the fast Fourier transform," *Biomaterials*, vol. 27, no. 32, pp. 5524–5534, 2006.

[11] C. E. Ayres, G. L. Bowlin, R. Pizinger, L. T. Taylor, C. A. Keen, and D. G. Simpson, "Incremental changes in anisotropy induce incremental changes in the material properties of electrospun scaffolds," *Acta Biomaterialia*, vol. 3, no. 5, pp. 651–661, 2007.

[12] D. Newton, R. Mahajan, C. Ayres, J. R. Bowman, G. L. Bowlin, and D. G. Simpson, "Regulation of material properties in electrospun scaffolds: role of cross-linking and fiber tertiary structure," *Acta Biomaterialia*, vol. 5, no. 1, pp. 518–529, 2009.

[13] D. I. Zeugolis, S. T. Khew, E. S. Y. Yew et al., "Electro-spinning of pure collagen nano-fibres—just an expensive way to make gelatin?" *Biomaterials*, vol. 29, no. 15, pp. 2293–2305, 2008.

[14] S. Heydarkhan-Hagvall, K. Schenke-Layland, A. P. Dhanasopon et al., "Three-dimensional electrospun ECM-based hybrid scaffolds for cardiovascular tissue engineering," *Biomaterials*, vol. 29, no. 19, pp. 2907–2914, 2008.

[15] L. Yang, C. F. C. Fitié, K. O. van der Werf, M. L. Bennink, P. J. Dijkstra, and J. Feijen, "Mechanical properties of single electrospun collagen type I fibers," *Biomaterials*, vol. 29, no. 8, pp. 955–962, 2008.

[16] D. G. Simpson, L. Terracio, M. Terracio, R. L. Price, D. C. Turner, and T. K. Borg, "Modulation of cardiac myocyte phenotype in vitro by the composition and orientation of the extracellular matrix," *Journal of Cellular Physiology*, vol. 161, no. 1, pp. 89–105, 1994.

[17] A. E. Manis, J. R. Bowman, G. L. Bowlin, and D. G. Simpson, "Electrospun nitrocellulose and nylon: design and fabrication

of novel high performance platforms for protein blotting applications," *Journal of Biological Engineering*, vol. 1, article 2, 2007.

[18] S. Weiner and W. Traub, "Organization of hydroxyapatite crystals within collagen fibrils," *FEBS Letters*, vol. 206, no. 2, pp. 262–266, 1986.

[19] I. V. Yannas, "Regeneration templates," in *The Biomedical Engineering Handbook*, J. D. Bronzino, Ed., CRC press LLC, Fla, USA, 2000.

[20] M. V. Agrez, R. C. Bates, A. W. Boyd, and G. F. Burns, "Arg-Gly-Asp-containing peptides expose novel collagen receptors on fibroblasts: implications for wound healing," *Cell Regulation*, vol. 2, no. 12, pp. 1035–1044, 1991.

[21] G. E. Davis, "Affinity of integrins for damaged extracellular matrix: Alpha v beta 3 binds to denatured collagen type I through RGD sites," *Biochemical and Biophysical Research Communications*, vol. 182, no. 3, pp. 1025–1031, 1992.

[22] D. A. Cisneros, C. Hung, C. M. Franz, and D. J. Muller, "Observing growth steps of collagen self-assembly by time-lapse high-resolution atomic force microscopy," *Journal of Structural Biology*, vol. 154, no. 3, pp. 232–245, 2006.

[23] K. R. Stevens, N. J. Einerson, J. A. Burmania, and W. J. Kao, "In vivo biocompatibility of gelatin-based hydrogels and interpenetrating networks," *Journal of Biomaterials Science*, vol. 13, no. 12, pp. 1353–1366, 2002.